Searching for Monomeric Nickel Tetrafluoride: Unravelling Infrared Matrix Isolation Spectra of Higher Nickel Fluorides

Lin Li, Ahmed K. Sakr, Tobias Schlöder, Siri Klein, Helmut Beckers, Marios-Petros Kitsaras, Howard V. Snelling, Nigel A. Young,* Dirk Andrae, and Sebastian Riedel*

Dedicated to Prof. Dieter Lentz on the occasion of his 70th birthday

Abstract: *Binary transition metal fluorides are textbook examples combining complex electronic features with most fundamental molecular structures. High-valent nickel fluorides are among the strongest known fluorinating and oxidizing agents, but there is a lack of experimental structural and spectroscopic investigations on molecular NiF_3 or NiF_4. Apart from their demanding synthesis, also their quantum-chemical description is difficult due to their open shell nature and low-lying excited electronic states. Distorted tetrahedral NiF_4 (D_{2d}) and trigonal planar NiF_3 (D_{3h}) molecules were produced by thermal evaporation and laser ablation of nickel atoms in a fluorine/noble gas mixture and spectroscopically identified by a joint matrix-isolation and quantum-chemical study. Their vibrational band positions provide detailed insights into their molecular structures.*

Binary fluorides of the late 1st row transition metals (TM) are among the most efficient oxidative fluorinating agents, especially for the production of perfluorinated organic

compounds.[1] CoF_3 is of industrial importance in the Flutec or Fowler processes,[2] and higher nickel fluorides are considered to be the active fluorinating agents in the electro-chemical fluorination of organic substrates (Simons process).[3] Despite numerous attempts to elucidate this latter process the active species are still unknown.[3,4]

Clearly, these particular properties are related to the peculiar electronic structure of these late TM fluorides, such as high ionization energies, the occupation of M−F antibonding molecular orbitals, and the lack of the so-called "primogenic repulsion", caused by the absence of radial nodes in the 3*d* valence orbitals.[5] Nickel is one of the most electronegative metallic elements.[6] This implies a considerable covalent character of the Ni−F bonds, which increases with the oxidation state of nickel.[7,8] Particularly for high-valent 3*d* TM complexes the similar radial extent of the 3*d* valence and the 3*p* core shell leads to repulsion between core 3*p* and ligand valence electrons, which ultimately results in weakened metal-ligand bonds,[5] a weak ligand-field, and the presence of several low-lying excited electronic (spin) states.[9] Taken together, these circumstances represent a challenge for quantum-chemical predictions and a major impediment for the spectral analysis of the still elusive high-valent molecular nickel fluorides.

In addition to the trifluorides, the tetrafluorides of the 1st row TM are particularly interesting. Solid MnF_4 releases elemental fluorine at temperatures $> 170\,°C$.[10] It can be used for storage and purification of elemental fluorine.[2] In contrast to solid MnF_4 and NiF_4, solid FeF_4 or solid CoF_4 are unknown, while the monomeric FeF_4 and CoF_4 species have been investigated by high-temperature vapor-phase mass spectrometry and cryogenic matrix-isolation spectroscopy.[11–13]

Solid NiF_4 is one of the strongest known fluorinating oxidizing agents,[2] but it is poorly characterized spectroscopically and even its solid-state structure is unknown. We have not found any report on molecular or gaseous NiF_4.[4] Fluorination of solid NiF_2 provides thermally unstable higher nickel fluorides such as Ni_2F_5 ($Ni^{II}_3Ni^{IV}F_{10}$)[14] or R-NiF_3 ($Ni^{II}Ni^{VI}F_6$),[15] and neutral NiF_4 is claimed to be formed at about $-60\,°C$ by treating $[NiF_6]^{2-}$ salts in anhydrous HF with strong Lewis acids such as AsF_5, SbF_5, or BF_3.[16] NiF_4 releases F_2 above $-55\,°C$ and forms NiF_3, which again releases fluorine above $20\,°C$ to form NiF_2.[17] As far as we know molecular NiF_3 has not yet been studied spectroscopically, but it has attracted the interest of a theoretical study because of

[*] M. Sc. L. Li, S. Klein, Dr. H. Beckers, Prof. Dr. S. Riedel
Freie Universität Berlin, Institut für Chemie und Biochemie—
Anorganische Chemie
Fabeckstrasse 34/36, 14195 Berlin (Germany)
E-mail: s.riedel@fu-berlin.de

Dr. A. K. Sakr, Dr. N. A. Young
Department of Chemistry and Biochemistry, University of Hull
Kingston upon Hull, HU6 7RX (UK)
E-mail: n.a.young@hull.ac.uk

Dr. T. Schlöder
Karlsruher Institut für Technologie, Institut für Nanotechnologie
Hermann-von-Helmholtz-Platz 1, 76344 Eggenstein-Leopoldshafen
(Germany)

M. Sc. M.-P. Kitsaras, Priv.-Doz. Dr. D. Andrae
Freie Universität Berlin, Institut für Chemie und Biochemie—
Theoretische Chemie
Arnimallee 22, 14195 Berlin (Germany)

Dr. H. V. Snelling
Department of Physics and Mathematics, University of Hull
Kingston upon Hull, HU6 7RX (UK)

its low-lying electronically degenerate excited states, which are prone to Jahn–Teller (JT) effects.[18]

We carried out spectroscopic investigations on molecular NiF_3 and NiF_4 for the first time. Different methods were applied to produce these species which were subsequently isolated in cryogenic rare-gas matrices. First, nickel atoms were vaporized by heating a nickel wire and allowed to react with elemental fluorine diluted in argon prior to deposition on a matrix support at 10 K. Vaporization of atomic nickel was also achieved by laser ablation using the 1064 nm fundamental of a Nd:YAG laser focused onto a rotating nickel target and trapping the products at 6–15 K. The laser ablation process is associated with a hot plasma plume and a bright broad-band radiation, where excited nickel atoms can react with elemental fluorine and atomic fluorine radicals seeded in excess of noble gases (neon or argon). This method is particularly useful for the generation of highly fluorinated species.[13,19] For example, laser ablation from a metallic cobalt target in a fluorine/argon gas mixture clearly produces not only molecular CoF, CoF_2 and CoF_3 but also CoF_4 (for experimental details see the Supporting Information), which could be detected using its known IR band in solid argon reported in a previous study,[12] in which CoF_4 was obtained at 650 K from solid mixtures of CoF_3 and TbF_4 as atomic fluorine source in a perfluorinated nickel effusion cell.[12] The wavenumber ordering of the ν_{Co-F} modes is $CoF_4 > CoF_3 > CoF_2 \gg CoF$, see the Supporting Information.

Thermally evaporated Ni atoms react with F_2 on deposition (Figure 1) to yield limited amounts of NiF_2 at 779.4 cm^{-1}[20] and a broad band at 625.8 cm^{-1} assigned to molecular NiF on the basis of the gas-phase IR band of ^{58}NiF ($^2\Pi_{3/2}$) at 634.7 cm^{-1},[21] and our computed value of 639.1 cm^{-1} at the CCSD(T)/AVT(Q)Z-DK level (Table S4.2). UV and broadband photolysis, associated with the formation of F radicals, resulted in the dramatic growth of the bands due to NiF_2 (Figure 1 (a,d)), and two additional sets of overlapping bands close to 800 cm^{-1}. Like the NiF_2 bands the well resolved

Scheme 1. Structures of NiF$_n$ (n = 1–4) species. Values calculated at the RCCSD(T)/AVTZ(NREL) and the RCCSD(T)/AVTZ-DK (in bold) levels of theory. [a] Experimental value from a gas phase electron diffraction study.[23] [b] CASPT2/AVTZ-DK.

^{58,60}Ni isotopic pattern on the 800 cm^{-1} bands is consistent with linear NiF_2 units (Table S3.1).[22] These new bands were assigned to matrix sites of NiF_2 in F_2/Ar matrices (see the Supporting Information).

On annealing (Figure 1 (b,c)), the bands due to NiF_2 increased while those close to 800 cm^{-1} decreased, and weak bands at 735–724 cm^{-1} appeared. These latter bands are assigned to the asymmetric stretch of molecular NiF_3, trapped in different matrix sites. CCSD(T) calculations predict a $^4A_2'$ ground state with D_{3h} structure for molecular NiF_3 (Scheme 1, Table S6.3) and a single infrared active E′ stretching fundamental about 40 cm^{-1} below that of NiF_2 (Table S6.4).

Subsequent nickel laser ablation experiments fully corroborate the assignment of NiF_3 in solid argon (Figure 2). Due to the formation of considerably larger amounts of atomic fluorine radicals in the laser ablation experiment, the yield of NiF_3 increased and further rose by annealing the deposit to 20 K (Figure 2). The NiF_3 region is even more congested in
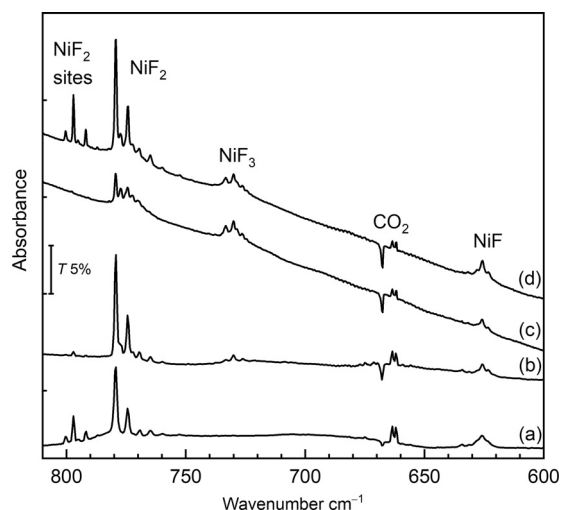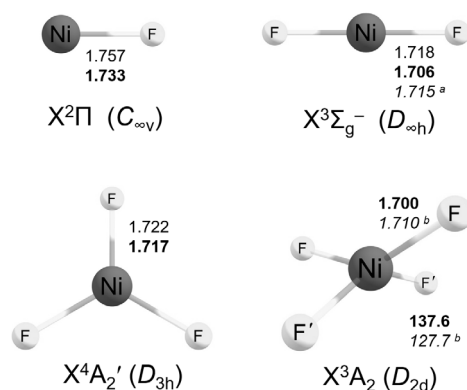

Figure 1. IR spectra of reaction products from thermally evaporated Ni atoms in 0.5% F_2/Ar matrices: a) after deposition and broadband photolysis, b) after annealing to 25 K, c) after deposition and annealing to 25 K, d) after broadband photolysis.
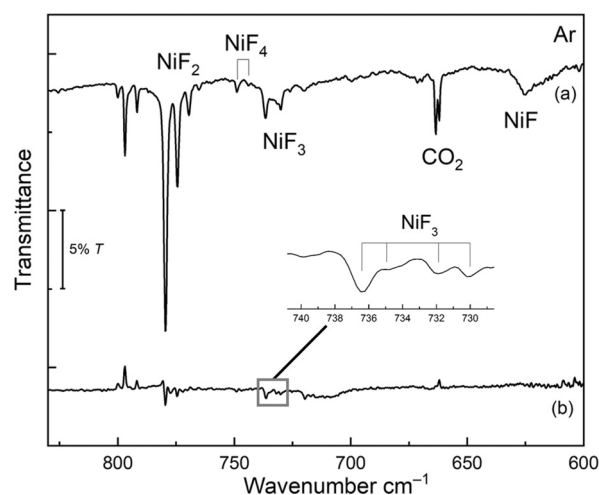
Figure 2. IR spectrum of the reaction products of laser-ablated Ni with F_2 (0.5%) seeded in excess argon: a) co-deposited for 60 min at 15 K, b) difference spectrum after annealing to 20 K.

the laser ablation experiment due the presence of different matrix sites. UV radiation of $\lambda = 273$ nm (LED) depletes the NiF_3 bands (band points upwards in Figure S4b) and forms NiF_2, while $\lambda = 193$ nm laser radiation destroyed both, NiF_2 and NiF_3 (Figure S4d). More interestingly, in these experiments a new band at 749.1 cm^{-1} with a distinct $\Delta v(^{58/60}Ni)$ isotope splitting of 5.1 cm^{-1} occurred (Figure 2). This band was very difficult to detect in the thermal evaporation experiment due to its much lower intensity. The carrier of this band appears to be formed by fluorination of NiF_3, since it can only be observed when a sufficient amount of NiF_3 is available and its intensity grows along with that of the NiF_3 band, i.e. by annealing and with higher fluorine concentrations of the F_2/Ar mixture (Figure S5). Based on this behavior, the new band is assigned to the strongest IR band of molecular NiF_4. For a tetrahedral tetrafluoride only a single infrared-active Ni–F stretching mode is expected, however, for the d^6 electronic configuration of NiF_4 a Jahn–Teller distorted D_{2d} structure is predicted at all levels of theory (Figure S7.1).

We are not aware of previous high-level ab initio calculations for molecular NiF_4. We carried out quantum-chemical investigations of various energetically low-lying electronic states of NiF_4, especially of the lowest-energy triplet ($^3A_2$) and quintet ($^5B_1$, $^5A_1$) states of D_{2d} symmetry (Table S3.4). For the triplet ground state (Scheme 1) a strong IR band of E symmetry is predicted for NiF_4 about 11 cm^{-1} blue-shifted from the E′ band of NiF_3 at the CCSD(T)/AVTZ-DK level (Table 1), which is in excellent agreement with the observation. The much weaker predicted B_2 band of NiF_4 (Tables S7.2, S7.4, S7.6) was not detected. All four nickel fluorides are also observed in solid neon matrices (Tables 1, S3.3).

A comparison of experimental M–F stretching bands of high-valent first-row metal fluorides is particularly revealing. The molecular trifluorides of M = Fe, Co, and Ni all adopt D_{3h} structures, and their stretching fundamentals were found in Ne matrices, in a very narrow range, at 743.6 cm^{-1} (Fe),[13] 748.2 cm^{-1} (Co), and 743.8 cm^{-1} (Ni, Table 1). For a series of molecules with similar structures one expects a strong correlation between stretching frequencies and bond lengths, a trend that also applies to the bond length of CoF_3 (1.722 Å) and NiF_3 (1.722 Å, Table S3.5) obtained at the CCSD(T)/AVTZ level. A similar frequency-bond length

correlation (Table S3.5) is expected for the stretching vibrations of the tetrafluorides MF_4 of Fe to Ni observed in solid argon, which also appear in a narrow spectral range (757 cm^{-1} (M = Fe),[13] 767.8 (Co),[12] 749.1 (Ni)). However, this correlation is less accurate due to the Jahn–Teller deformed D_{2d} molecular structures of FeF_4 and NiF_4 and due to stronger matrix interactions in solid argon.

Apart from these similarities, the higher nickel fluorides are strikingly different from their third-row predecessors. The rule of thumb that higher fluorides have shorter and stronger M–F bonds that applies to ionic metal fluorides does not apply to the higher nickel fluorides. While CCSD(T)/AVTZ calculations predict a successive M–F bond shortening for the ionic iron fluorides FeF_n, with $n = 1$–4,[13] and, albeit significantly weakened, also for CoF_n, $n = 2$–4, the bond length in NiF_n, $n = 2$–4, remains almost unchanged (Table S3.5). This different trend for nickel and its predecessors can be traced back to fundamental aspects of their atomic structures, such as a higher nickel ionization energy. This leads to a considerable covalent character of the Ni–F bonds, associated with a low-spin triplet electronic ground-state of NiF_4 and a considerable radical character of the fluorine ligands (Figure S11).[7,8]

From these experiments we conclude that NiF_2, initially formed from the reaction of nickel atoms and elemental fluorine, can be regarded as chemically inert to elemental fluorine, but reacts rapidly with atomic fluorine radicals to

Table 2: Calculated thermochemistry of nickel fluorides in kJ mol^{-1}.

	$\Delta E°$ (kJ mol^{-1}), CCSD(T)/AVTZ-DK
Ni + F → NiF	−426.16
NiF + F → NiF_2	−507.44
NiF + F_2 → NiF_3	−517.91
NiF_2 + F → NiF_3	−163.50
NiF_3 + F → NiF_4	−76.04

form NiF_3 and further to NiF_4. It has also been shown that the reaction of Ni atoms with elemental F_2 to produce NiF_2 requires UV photolysis to yield appreciable quantities of product under the cryogenic conditions applied here. Given the highly exothermic reaction energy of this reaction

Table 1: Vibrational frequencies observed in laser-ablation experiments and computed harmonic frequencies (in cm^{-1}) for NiF_n ($n = 1$–4).

Species	Ground State	Sym.	calcd[a]		Exp. (Ne Matrix)		Exp. (Ar Matrix)	
			^{58}Ni	^{60}Ni	^{58}Ni	^{60}Ni	^{58}Ni	^{60}Ni
NiF	$^2\Pi$	$C_{\infty v}$	NR[b] 612.98 (Σ^+)	610.46	646.2	643.5	625.8 (broad)	
			DK[b] 639.13 (Σ^+)	636.50				
NiF_2	$^3\Sigma_g^-$	$D_{\infty h}$	NR[c] 806.42 (Σ_u^+)	801.09	800.1	794.9	779.5	774.4
			DK[c] 819.17 (Σ_u^+)	813.75				
			NR[b] 810.25 (Σ_u^+)	804.89				
			DK[b] 824.62 (Σ_u^+)	819.17				
NiF_3	$^4A_2'$	D_{3h}	NR[c] 762.95 (E′)	758.67	743.8	740.0	736.5	731.7
			DK[c] 767.83 (E′)	763.54				
NiF_4	$^3A_2$	D_{2d}	NR[c] 767.24 (E)	762.56	762.3	757.2	749.1	744.0
			DK[c] 778.50 (E)	773.71				

[a] Non-relativistic (NR) and with scalar-relativistic Douglas-Kroll-Hess (DK) Hamiltonian; [b] RCCSD(T)/AVQZ; [c] RCCSD(T)/AVTZ.

(Table 2), this observation indicates a considerable reaction barrier and the necessity for fluorine radicals.

To summarize, molecular NiF_4 (D_{2d}) and NiF_3 (D_{3h}) were produced, isolated in solid noble-gas matrices, and spectroscopically identified aided by quantum-chemical calculations. Their weak Ni−F bonds and a considerable fluorine radical character make these molecular species very powerful fluorination and oxidation agents.

Acknowledgements

Conflict of interest

The authors declare no conflict of interest.

[1] P. Kirsch, *Modern Fluoroorganic Chemistry. Synthesis Reactivity, Applications*, Wiley-VCH, Weinheim, **2004**, pp. 25–33.

[2] A. Higelin, S. Riedel in *Modern Synthesis Processes and Reactivity of Fluorinated Compounds. Progress in Fluorine Science* (Eds.: H. Groult, F. Leroux, A. Tressaud), Elsevier Science, San Diego, **2016**, pp. 561–586.

[3] S. Mattsson, G. Senges, S. Riedel, B. Paulus, *Chem. Eur. J.* **2020**, *26*, 10781.

[4] M. I. Nikitin, A. S. Alikhanyan, *Russ. J. Inorg. Chem.* **2020**, *65*, 199.

[5] a) P. Pyykkö, *Chem. Rev.* **1988**, *88*, 563; b) M. Kaupp, *J. Comput. Chem.* **2007**, *28*, 320.

[6] a) M. Rahm, T. Zeng, R. Hoffmann, *J. Am. Chem. Soc.* **2019**, *141*, 342; b) J. B. Mann, T. L. Meek, E. T. Knight, J. F. Capitani, L. C. Allen, *J. Am. Chem. Soc.* **2000**, *122*, 5132.

[7] G. L. Gutsev, A. I. Boldyrev, *Int. J. Mass Spectrom. Ion Processes* **1989**, *91*, 135.

[8] P. J. Leszczyński, W. Grochala, *Acta Chim. Slov.* **2013**, *60*, 455.

[9] J. K. McCusker, *Science* **2019**, *363*, 484.

[10] F. Kraus, S. I. Ivlev, J. Bandemehr, M. Sachs, C. Pietzonka, M. Conrad, M. Serafin, B. G. Müller, *Z. Anorg. Allg. Chem.* **2020**, *646*, 1481.

[11] a) J. V. Rau, S. Nunziante Cesaro, N. S. Chilingarov, M. S. Leskiv, G. Balducci, L. N. Sidorov, *Inorg. Chem. Commun.* **2003**, *6*, 643; b) E. L. Osina, N. S. Chilingarov, S. B. Osin, E. V. Skokan, M. I. Nikitin, *Russ. J. Phys. Chem. A* **2019**, *93*, 185.

[12] J. V. Rau, S. Nunziante Cesaro, N. S. Chilingarov, G. Balducci, *Inorg. Chem.* **1999**, *38*, 5695.

[13] T. Schlöder, T. Vent-Schmidt, S. Riedel, *Angew. Chem. Int. Ed.* **2012**, *51*, 12063; *Angew. Chem.* **2012**, *124*, 12229.

[14] M. Tramšek, B. Žemva, *Acta Chim. Slov.* **2002**, *49*, 209.

[15] C. Shen, L. C. Chacón, N. Rosov, S. H. Elder, J. C. Allman, N. Bartlett, *C. R. Acad. Sci. Paris Ser. II C* **1999**, *2*, 557.

[16] a) N. Bartlett, R. D. Chambers, A. J. Roche, R. C. H. Spink, L. Chacón, J. M. Whalen, *Chem. Commun.* **1996**, 1049; b) T. L. Court, M. F. A. Dove, *J. Chem. Soc. D* **1971**, 726; c) B. Zemva, K. Lutar, A. Jesih, W. J. Casteel, N. Bartlett, *J. Chem. Soc. Chem. Commun.* **1989**, 346.

[17] B. Zemva, K. Lutar, L. Chacón, M. Fele-Beuermann, J. Allman, C. Shen, N. Bartlett, *J. Am. Chem. Soc.* **1995**, *117*, 10025.

[18] a) P. Mondal, D. Opalka, L. V. Poluyanov, W. Domcke, *J. Chem. Phys.* **2012**, *136*, 084308; b) P. Mondal, W. Domcke, *J. Phys. Chem. A* **2014**, *118*, 3726.

[19] F. Brosi, T. Schlöder, A. Schmidt, H. Beckers, S. Riedel, *Dalton Trans.* **2016**, *45*, 5038.

[20] a) D. E. Milligan, M. E. Jacox, J. D. McKinley, *J. Chem. Phys.* **1965**, *42*, 902; b) D. A. van Leirsburg, C. W. DeKock, *J. Phys. Chem.* **1974**, *78*, 134; c) J. W. Hastie, R. H. Hauge, J. L. Margrave, *J. Chem. Soc. D: Chem. Comm.* **1969**, 1452; d) J. W. Hastie, R. H. Hauge, J. L. Margrave, *High Temp. Sci.* **1969**, *1*, 76.

[21] D. L. Arsenault, D. W. Tokaryk, A. G. Adam, C. Linton, *J. Mol. Spectrosc.* **2016**, *324*, 20.

[22] O. M. Wilkin, N. Harris, J. F. Rooms, E. L. Dixon, A. J. Bridgeman, N. A. Young, *J. Phys. Chem. A* **2018**, *122*, 1994.

[23] N. Vogt, *J. Mol. Struct.* **2001**, *570*, 189.